EUROPEAN COMMISSION
5th EURATOM FRAMEWORK PROGRAMME 1998-2002
KEY ACTION : NUCLEAR FISSION

HTR-E

High-Temperature Reactor Components and Systems

CONTRACT N°
FIKI-CT-2001-00177

WP1

Helium Turbine Design Study

Deliverable n°10a

René A. Van den Braembussche

von Karman Institute

Belgium

Dissemination level : RE
Document N°: HTR-E 05/06 D-1-2-3-1/2
Status : Final
Deliverable n°10a

von Karman Institute for Fluid Dynamics
Waterloose steenweg, 72
B-1640 SINT-GENESIUS-RODE, BELGIUM.

CONTRACT N°
FIKI-CT-2001-00177

WP1

Helium Turbine Design Study

Deliverable n°10a

René A. Van den Braembussche

von Karman Institute

Belgium

Ref:	VKI CR 2005-46
Date	June 6, 2005
Approved	Rene Van den Braembussche
Visa	

HTR-E WP1 - INTRODUCTION
-

High investment cost and/or important safety issues may impose the need for experimental verifications before manufacturing and assembling the full-scale plant.

The high cost of full scale prototype testing enhances the importance of studying the possibility of scale model testing. Smaller models are not only much cheaper but also allow rapid verifications of modifications and corrections of the lay out before building the full scale machine. In what follows one will give a short overview of the theory and flow models that govern the steady operation and the transient changes of the flow in the gasturbine. By analyzing these models it will become possible to define the conditions and similarity rules that must be respected when defining the scaled model in order to guarantee that the experimental results are representative for the full size device.

Features that could be verified in this way are:

1. The steady performance of each component. This is important because of the direct impact on cycle efficiency and is needed to define the steady operating point of the complete gasturbine. The performance of each component (compressor and turbine) and the interaction defining the operating point is described in PART I.

2. The unsteady interaction between each component in the circuit. This is needed to verify that the start- and stop procedure, the variations in operating point or emergency actions will not generate unacceptable mechanical solicitations that could damage the components. In particular one may want to avoid surge and stall, excessive overspeed of the rotating components or overheating and thermal shocks. The theory to model the performance at varying (unsteady) conditions is described in PART II.

3. The possibility to do some component testing in Helium in the HTR-10GT facility under construction by INET at the Tsinghua University, or to extrapolate the results of the component performance measurements to present application is discussed in PART III.

PART I – STEADY GASTURBINE PERFORMANCE EVALUATIONS

1. Compressor and Turbine performance scaling

Compressor and turbine performance are governed by the change in flow direction (work input), diffusion or acceleration, Mach number level (compressibility effects) and Reynolds number (ratio between friction and inertial forces). It can be shown that, when conserving the value of these terms, the performance (pressure ratio and efficiency) will be unchanged and that the impact of a dimensional scaling on mass flow can be evaluated easily. However, one should keep in mind that a dimensional scaling not only concerns the dimensions of blades and casing but all geometrical parameters inclusive the clearance, roughness etc..

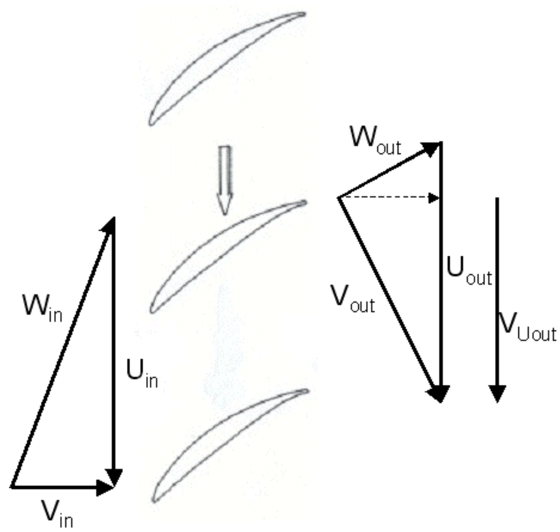

Fig. 1 Velocity triangles

Conservation of velocity triangles and Mach number means that both fluid and mechanical velocities must be scaled by the speed of sound $a = \sqrt{\gamma . R_G . T}$ (Fig. 1). Scaling the peripheral velocity with the speed of sound means that, at unchanged dimensions and fluid properties, the RPS should vary in function of the square root of the inlet temperature

$$RPS = RPS_{ref} \cdot \sqrt{T_{in} / T_{in,ref}} \qquad (1)$$

The mass flow being a function of the axial velocity and density of the fluid, one can define it in function of the mass flow at reference inlet conditions by correcting for the density and velocity changes.

$$\dot{m} = \dot{m}_{ref} \frac{P}{R_G.T}\left(\frac{R_G.T}{P}\right)_{ref}\sqrt{\frac{T}{T_{ref}}} = \dot{m}_{ref} P / P_{ref} / \sqrt{T / T_{ref}}$$

which is commonly written as

$$\dot{m} = \dot{m}_{ref}\delta / \sqrt{\theta}$$

where $\delta = P / P_{ref}$ and $\theta = T / T_{ref}$

In case of geometrical scaling the mass flow also scales with the inlet section i.e. square of the geometrical scale factor.

$$\dot{m} = \dot{m}_{ref}\delta / \sqrt{\theta}\,\left(R_{in} / R_{in,ref}\right)^2 \qquad (2)$$

The outlet over inlet pressure ratio is defined by:

$$\pi = 1 + \Delta P / P_{in} \qquad (3)$$

ΔP stands for P_{out}-P_{in} and can also be written as $\rho.\ \Delta H$
where $\Delta H = U_{out}.V_{Uout}-U_{in}.V_{Uin}$ (Fig. 1) is the specific entalpy rise and proportional to U^2_2 . The velocities scale with the speed of sound and ΔH is thus proportional to T_{in} . Hence the pressure increase ΔP is proportional to $\rho.T$ which can also be written as $\Delta P \approx \frac{P}{R_G.T} T \approx P$. As a result, the pressure ratio is independent of inlet pressure and temperature, if the *RPS* has been adapted according to eq. (1).

This procedure can be used to calculate the compressor and turbine performance at reference conditions (Fig. 2a and b) starting from measurements at any conditions. It can also be used to calculate the compressor and turbine performance at any operating conditions starting from the information contained in Fig. 2a and b. The turbine mass flow on Fig. 2b has been multiplied by RPS_{ref} to avoid that all speed lines fall so closely together that one can not distinguish between them.

The lower values of RPS_{ref}. for turbines than for compressors do not result from a difference in mechanical *RPS* between compressor and turbine but from the fact that turbines generally operate at much higher inlet temperatures ($T^0{}_{in}$) than compressors.

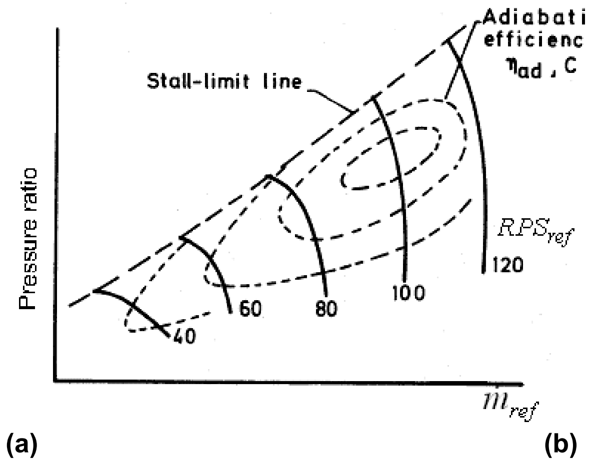

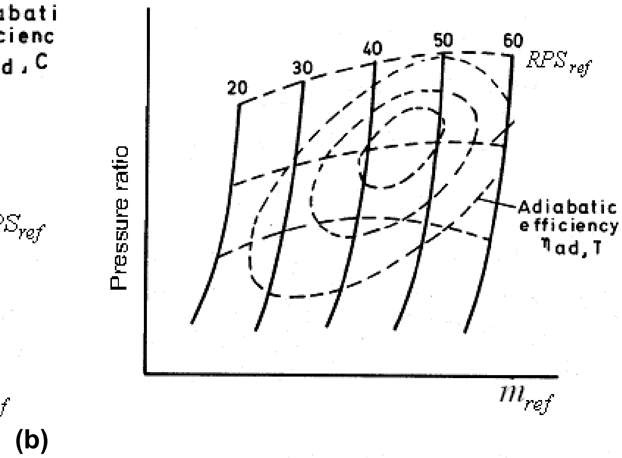

Fig. 2 Compressor (a) and Turbine (b) operating map at reference conditions

The compressor power absorption and turbine power delivery are defined by (KW)

$$KW_{comp}(\dot{m}_C) = \dot{m}_C\, C_p\, \Delta T_{comp}(\dot{m}_C) = \dot{m}_C\, C_p\ \ T^0{}_1 \frac{\left(P_2(\dot{m})/P_1(\dot{m})\right)^{\frac{\gamma-1}{\gamma}} - 1}{\eta} \tag{4a}$$

$$KW_{turb}(\dot{m}_T) = \dot{m}_T\, C_p\, \Delta T_{turb}(\dot{m}_T) = \dot{m}_T\, C_p\ \ T^0{}_3\ \eta\ \left(1 - \left(P_4(\dot{m})/P_3(\dot{m})\right)^{\frac{\gamma-1}{\gamma}}\right) \tag{4b}$$

Specific Power is the power per unit mass flow , non-dimensionalized by RPS^2. Typical values are shown on Fig. 3.

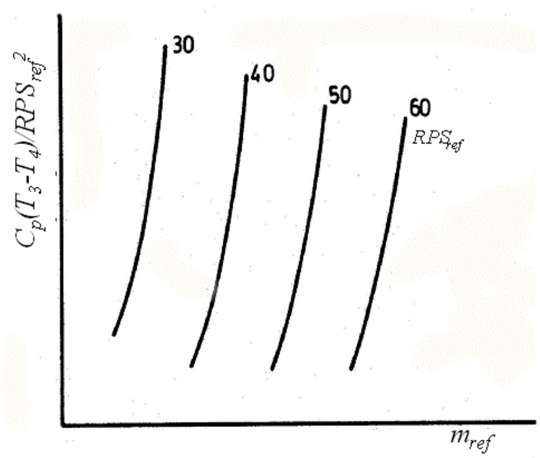

Fig. 3 Turbine Specific Power versus reference mass flow

Previous equations have been used to define the geometry and test conditions for a down-scaled model of the compressor and turbine and to define the test conditions allowing an accurate experimental evaluation of the performance map.

1.1 Use of a scale model for turbine performance evaluation

The scaling is based on the characteristics of helium and air, listed in table 1

Table 1 Gas-constants

	γ	R_G	C_P	μ
helium	1.666	2078	5196	$45.0\ 10^{-6}$
air	1.4	285	1005	$17.2\ 10^{-6}$

Starting point is the 12 stage helium turbine of diameter *1.9 m* rotating at *3000. RPM* with inlet temperature $T^0{}_3$*=1121.2.* ^oK and inlet pressure of *7 Mpa*. [8]. Tests could be performed at *393.* ^oK inlet temperature and *200 000. Pa* inlet pressure. Based on the ratio between the corresponding speed of sound in air (*396 m/s*) and in helium (*1970 m/s*) all velocities should be reduced by a factor *4.97* . Assuming that the scaled model rotates in air at *1000 RPM* instead of *3000 RPM* for the helium turbine, one obtains that the Mach numbers and velocity triangles are conserved if the diameter scales as follows:

$$D_{air} = \frac{1.9\ \ 3000.\ \sqrt{1.4\ \ 285.\ \ 393.}}{1000.\sqrt{1.666\ \ 2078.\ \ 1121.2.}} = 1.145\ m$$

The outlet pressure is *116.5 kPa*, the mass flow is *13.83 kg/sec* and *959.4 kW* is required to drive the multistage compressor in air. The blade chord length reduces by the same scale factor from *.06 m* to *.0361 m.*

The losses depend on the Reynolds number based on blade chord length. A *.06 m* chord length in helium and a *.03618 m* chord length in air result in following values for the Reynolds number:

$$\mathrm{Re}_{He} = \frac{3000.\ \pi\ 1.9}{60}\ \frac{1}{45.0\ 10.^{-6}}\ \frac{7.\ 10.^6}{2078.\ 1121.2.}\ .06 = 1195\,587.$$

$$\mathrm{Re}_{Air} = \frac{1000.\ \pi\,1.145}{60}\ \frac{1}{17.2\ 10.^{-6}}\ \frac{2.*10.^5}{285.\ 393.}\ .03616 = 225\ \ 305\,.$$

The Reynolds number in air (*1000 RPM*) may approach the critical value of *100 000.* near the turbine exit where the pressure is 116 500. Pa. One can therefore not guarantee that the performance measured in air at 200 000. Pa inlet pressure will be representative for the that will be obtained in a larger turbine operating in helium at *7. MPa* inlet pressure. An increase of the air pressure at test conditions to *.5 MPa* would result in a 5 times larger Reynolds number *(Re= 563 264)* and guarantee an almost identical performance in air as in helium. However the power would raise to *2.4 MW* for a *34.6 Kg/sec* mass flow.

One could limit the testing to a few stages (instead of 12), which would reduce the power requirements proportionally.

Making the model tests at *3000 RPM* would result in a diameter of only *.382 m* and a chord length of *.0120 m*. The mass flow would be *1.54 kg/sec* and only *106.5 kW* would be needed to drive it. However this would not only create manufacturing problems but also prohibit relevant measurements because the Reynolds number would be *75 000* which is far below the critical value.

1.2 Use of scale model for compressor performance evaluation

The scaling is based on the same characteristics of helium and air, listed in table 1

Starting point is the LP helium compressor of diameter *1.8 m* rotating at *3000 RPM* with inlet temperature $T^0_1 = 293.\ {}^oK$ [8]. Based on the ratio between the corresponding speed of sound in air (*341.3 m/s*) and in helium (*1017. m/s*) all velocities should be reduced by a factor 2.98 . Assuming that the scaled model rotates at 1000 RPM instead of 3000 for the helium turbines one obtains that the Mach numbers and velocity triangles are conserved if the diameter is almost unchanged:

$$D_{air} = \frac{1.8\ \ 3000.\ \sqrt{1.4\ \ 285.\ \ 293.}}{1000.\sqrt{1.666\ \ 2078.\ \ 299.}} = 1.815\ m$$

This means that the full-scale compressor could be tested in air at *1000 RPM* without any modification. Keeping the rotational speed at *3000 RPM* would result in a diameter of only *.604 m* and a chord length of *.02 m*. This is about the limit of what is can be manufactured while maintaining the required tolerances.

The losses depend on the Reynolds number based on blade chord length. Testing the full scale compressor in air and helium results in following values for the Reynolds number:

$$\mathrm{Re}_{He} = \frac{3000.\ \pi\ 1.8}{60}\ \frac{1}{45.0\ \ 10.^{-6}}\ \frac{2.55.\ 10.^{6}}{2078.\ \ 299.}\ .06\ = 1\,547\,200\,.$$

$$\mathrm{Re}_{Air} = \frac{1000.\ \pi\, 1.81}{60}\ \frac{1}{17.2\ \ 10.^{-6}}\ \frac{10.^{5}}{285.\ \ 293.}\ .0604\ = 400\,196\,.$$

The Reynolds number in air is about four times smaller than the value in Helium but still well above the critical value. The performance measured in air at atmospheric inlet conditions on the full-scale compressor at *1000 RPM* will be representative for the one operating in helium at 70 bar inlet pressure.

Testing the compressor on a reduced scale model at 3000 RPM in air results in:

$$Re_{Air} = \frac{3000.\ \pi\, 0.604}{60}\ \frac{1}{17.2\ 10.^{-6}}\ \frac{10.^{5}}{285.\ 293.}.02\ = 133\,399\,.$$

The Reynolds number is now rather close to the critical value but the Reynolds number increases towards the later stages and tests will provide a performance that is not far from the full scale one in Helium. An increase of the inlet pressure would relieve the uncertainty here.

The mass flow in the full scale compressor operated in air at atmospheric inlet conditions is 31.69 kg/sec and 5.5 MW is needed to drive it. The small scale compressor operating at 3000 RPM requires only .61 MW to compress 3.52 kg/sec .

2. Steady operating conditions

The gasturbine operating point is defined by the equilibrium between the different components : i.e. the compressor, turbine, reactor or combustion chamber, piping, heat exchangers and eventually coolers. The piping, reactor, turbine and heat exchangers represent a resistance, a flow restriction or load to the compressor. The turbine drives the compressor and gasturbine load (electric power output). Any change in requested power output will be felt by the turbine requiring a change in thermodynamic cycle conditions. In an open cycle gasturbine this is achieved by a change in fuel flow, eventually in combination with a change in mass flow. In a closed cycle gasturbine it requires a change in heating by the reactor or heat exchanger eventually in combination with a change in inventory. The consequence for the compressor and turbine is a modified pressure ratio and mass flow and even a change in RPM , i.e. an other operating point.

In case the load is an electrical generator, the mechanical *RPM* is fixed and defined by the frequency of the net (max. 3000 *RPM* or 3600 *RPM*). Any change in turbine inlet conditions will result in a variation of the pressure drop and mass flow and hence a change in power output. The *RPM* being fixed, the variation of the compressor load is restricted to one operating curve and the increase or decrease of the turbine power output will be compensated by a variation of the electrical generator output. This simplifies the problem at normal operation because one does not have to account for the inertial terms related to changes in *RPM*. However inertia of the rotor will influence the change in *RPM* in case of accidental load release.

In what follows one will concentrate on the closed cycle configuration operating at fixed *RPM*. The compressor and turbine matching is more complicated for closed cycles because the pressure level is not constant. It depends as well on the operation conditions as on the amount of fluid in the circuit (inventory) and there is no location where a reference pressure (i.e. P_{atm}) can be imposed.

The matching of a compressor and turbine on a single spool closed cycle configuration at steady operating conditions, is based on the following conditions:

1. the fluid weight flow in de compressor must be equal to the one in the turbine, corrected for by-pass or internal leakage flow.
2. the pressure rise of the compressor equals the pressure drop in the turbine, corrected for friction losses in the reactor, heat exchangers and ducts,
3. the power output of the turbine equals the power absorbed by the compressor, the accessories and load.
4. the turbine and compressor have the same and constant mechanical speed, fixed by the electric generator. Deceleration will occur only if the turbine output power is lower than the compressor- and accessory power (except if negative load, i.e. driving the gasturbine, is applied).

In what follows one will describe the procedure for a simple single spool closed cycle gasturbine (Fig. 4) with one compressor (c), recuperator (d), reactor (e), turbine (f), generator (i), and cooler (b). The figure also shows a reservoir (l) where the fluid can be stored when changing the inventory. It is fed trough the valve (V3) and emptied trough the valve (V6). The system can easily be extended to more complex configurations by repeating some components (i.e. a second compressor with intercooler, etc..).

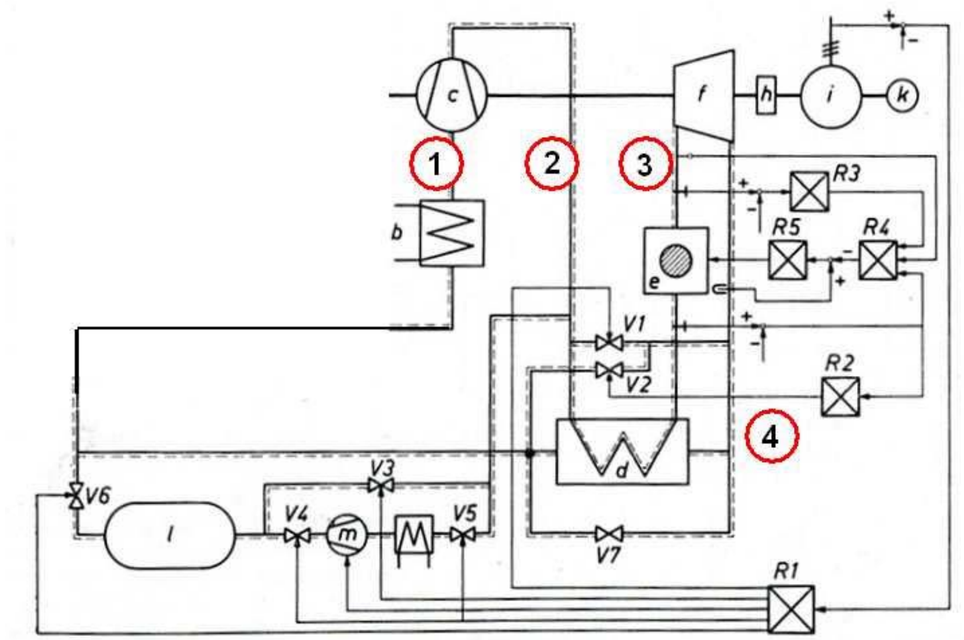

Fig. 4 Cycle layout

The main positions used in the subscripts are:

1	compressor inlet
2	compressor outlet
3	turbine inlet
4	turbine outlet

The first matching condition requires that:

$$\dot{m}_C(1-bleed)=\dot{m}_T \tag{5}$$

where bleed is the leakage flow in the bypass valve (V1 or V2).

The second condition results in:

$$\Delta P_{comp}-\Delta P^{HP}{}_{loss}=\Delta P_{turb}+\Delta P^{LP}{}_{loss} \tag{6}$$

$\Delta P^{HP}{}_{loss}$ are the pressure losses between the compressor exit (2) and turbine inlet (3) (ducts, cold part of recuperator, reactor). $\Delta P^{LP}{}_{loss}$ are the losses between the turbine exit (4) and the compressor inlet (1) (hot part of recuperator, valves and cooler). In what follows one will evaluate the pressure- and temperature change in each of these components as a function of the local inlet flow conditions and mass flow.

2.1 Compressor

Starting from a first guess of the compressor inlet pressure and temperature (P_1 and T_1) one can calculate the variation of $\Delta P_{comp}(\dot{m}_C)$ from the information on Fig. 2a for the speed line corresponding to the fixed mechanical RPM . Although the operation is at a constant mechanical RPM (3000 or 3600) one may have to take the performance from curves with different RPS_{ref} because it is function of the compressor inlet temperature.
The compressor outlet pressure is then easily defined for each mass flow

$$P_2(\dot{m})=P_1+\Delta P_{comp}(\dot{m}) \tag{7}$$

The temperature rise is function of the compressor efficiency, available also on Fig. 2a.

$$\Delta T_{com}(\dot{m}_C)=T^0{}_1\,\frac{\left(P_2(\dot{m})/P_1(\dot{m})\right)^{\frac{\gamma-1}{\gamma}}-1}{\eta}$$

$$T_2(\dot{m})=T_1+\Delta T_{comp}(\dot{m}_C) \tag{8}$$

The power needed to drive the compressor is defined by:

$$KW_{comp}(\dot{m}_C)=\dot{m}_C\,C_p\,\Delta T_{comp}(\dot{m}_C)=\dot{m}_C\,C_p\;T^0{}_1\,\frac{\left(P_2(\dot{m})/P_1(\dot{m})\right)^{\frac{\gamma-1}{\gamma}}-1}{\eta} \tag{9}$$

2.2 Ducts

$\Delta P^{HP}{}_{loss}$ stands for the friction losses in the ducts. The steady pressure losses due to friction in the ducts are defined by

$$\Delta P_{frict.} = C_f \ \rho \ V^2 \frac{L}{D_H} \tag{10}$$

where L is the length of the duct and D_H the hydraulic diameter of the duct defined by:

$$D_H = 4 \frac{Ar}{Cr}$$

Ar is the duct cross section area and Cr is the duct cross section contour length.

V is the average velocity and function of the mass flow, density and cross section area. It is given by:

$$V(\dot{m}) = \frac{\dot{m}}{Ar} \frac{R_G \, T(\dot{m})}{P(\dot{m})} \tag{11}$$

where $P(\dot{m})$ and $T(\dot{m})$ are local values averaged over the duct length. One can eventually split this loss calculation into 2 part:
* from the compressor exit to the bypass valve, where the mass flow is $\dot{m}_2$, and
* from the bypass valve to the turbine inlet where the mass flow is $\dot{m}_2(1-bleed)$

$$\Delta P_{frict.}(\dot{m}) = C_f \ \frac{\dot{m}^2}{Ar^2} \frac{L_H}{D_H} \frac{R_G \, T(\dot{m})}{P(\dot{m})} \tag{12}$$

This expression provides the pressure losses in function of the duct geometry, local mass flow, pressure, temperature and C_f . The latter one is the friction coefficient, function of the local Reynolds number and wall roughness [1].

The heat loss in the duct can be approximated by

$$Q(\dot{m}) = h \ \Delta T_{\ln} \ \frac{\pi D^2 L}{4} \tag{13}$$

where h is the heat transfer coefficient. Its value can be estimated from the Nusselt number, conductivity of the fluid (k) and hydraulic diameter D_H .

$$h = \frac{Nu \ k}{D_H} \tag{14}$$

The Nusselt number for the flow in a pipe can be estimated by the correlation of Dittus-Bölter [2]

$$Nu = .023 \ \mathrm{Re}_{D_H}{}^{0.8} \ \mathrm{Pr}^{0.3} \tag{15}$$

$$\mathrm{Re} = \frac{V \ D_H}{\mu} \rho = f(\dot{m}) \qquad\qquad \mathrm{Pr} = 0.7$$

$\Delta T_{\ln}$ is the logarithmic mean temperature difference, function of the fluid inlet (T_{in}) and outlet (T_{out}) temperature and the wall temperature (T_s).

Assuming constant wall temperature simplifies the problem and results in the following value of the logarithmic mean temperature difference:

$$\Delta T_{\ln} = \frac{T_{out} - T_{in}}{\ln \dfrac{T_{wall} - T_{out}}{T_{wall} - T_{in}}} \tag{16}$$

Hence the fluid temperature at the outlet of the duct is defined by:

$$T_{out} = T_{wall} - (T_{wall} - T_{in}) e^{\left(\frac{-h \frac{\pi D^2 L}{4}}{\dot{m} \ C_p} \right)} \tag{17}$$

2.3 Recuperator and coolers

The assumption of a constant wall temperature is an acceptable approximation for a water coolers where the wall temperature is close to the liquid temperature. The approach described in 2.2 for ducts may therefore be used also for water-coolers by imposing a constant wall temperature equal to the average water temperature. A typical variation of the difference between the cooler outlet gas temperature T^*_{out} and water inlet temperature T_{in} with amount of gas flow is shown on Fig. 5. It allows predicting the variation in outlet temperature with mass flow once the performance at design point is obtained.

Recuperators differ from coolers by the fact that the wall temperature can not be considered constant but depends on the temperature of the incoming flows i.e. temperature difference between the hot and cold fluid. The average logarithmic temperature difference of a counter-flow heat exchanger is given by

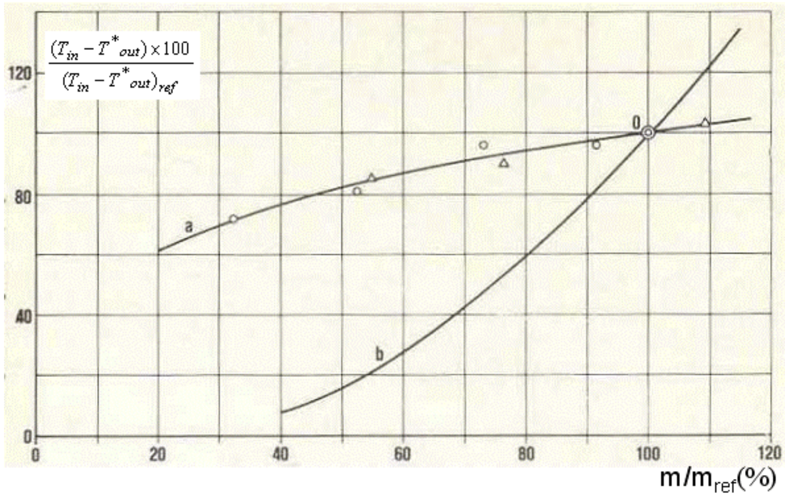

Fig. 5 Variation of cooler temperature difference with mass flow [3].

$$\Delta T_{\ln} = \frac{\left(T_{in} - T^*_{out}\right) - \left(T_{out} - T^*_{in}\right)}{\ln \dfrac{T_{in} - T^*_{out}}{T_{out} - T^*_{in}}} \tag{18}$$

Where T_{in} and T_{out} are the inlet and outlet temperature of the hot gas on the low pressure side (to be cooled) and T^*_{in} and T^*_{out} the inlet and outlet temperature of the cold gas on the high pressure side (to be heated).

The heat loss on the hot side being equal to the heat addition on the cold side, together with an adapted version of eq. (13), provides following relations

$$\dot{m}_{LP}\ C_{p,LP}\ (T_{in} - T_{out}) = h\ \Delta T_{\ln}\ Surf. \tag{19}$$

$$\dot{m}_{HP}\ C_{p,HP}\ (T^*_{out} - T^*_{in}) = h\ \Delta T_{\ln}\ Surf. \tag{20}$$

This allows defining the outlet temperature of both the HP (cold) and LP (warm) side as a function of the respective inlet temperatures, flow characteristics and mass flow. After substitution in (18), it allows the calculation of the heat transfer in the recuperator because $\Delta T_{\ln}$ is then function only of known $\dot{m}_{HP}$, $\dot{m}_{LP}$, T_1 and T^*_1.
The amount of heat exchange is

$$Q(\dot{m}) = h\ \Delta T_{\ln}\ surf. \tag{21}$$

The equation is useful to calculate the off design performance (reduced mass flow) once the value of h.Surf is known at design conditions. Fig.6 shows the difference in temperature between the outlet of the colder HP flow and the input of the hotter LP flow. It shows the decrease in temperature difference with decreasing flow [3] .

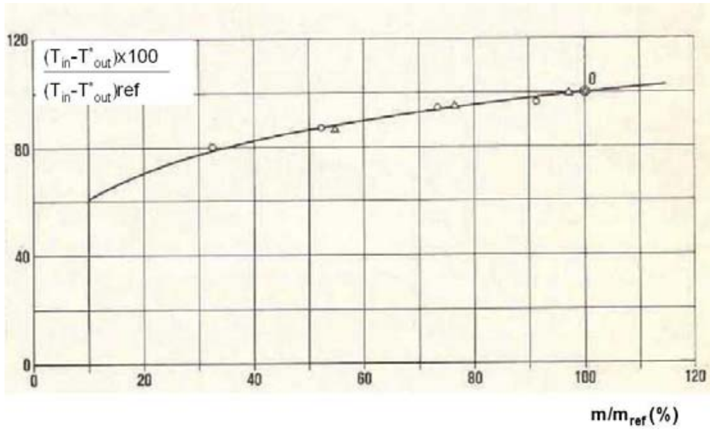

Fig. 6 Variation of temperature difference in recuperator [3].

2.4 Volumes

Large volumes, as observed in heat exchangers, reactors or combustion chambers, result in low velocities. Hence the friction losses may be very small or negligible. However, depending on the shape of the inlet and outlet, large kinetic energy losses, due to sudden expansion or acceleration, may occur at the inlet and outlet of the heat exchanger or reactor (Fig. 7 a and b).

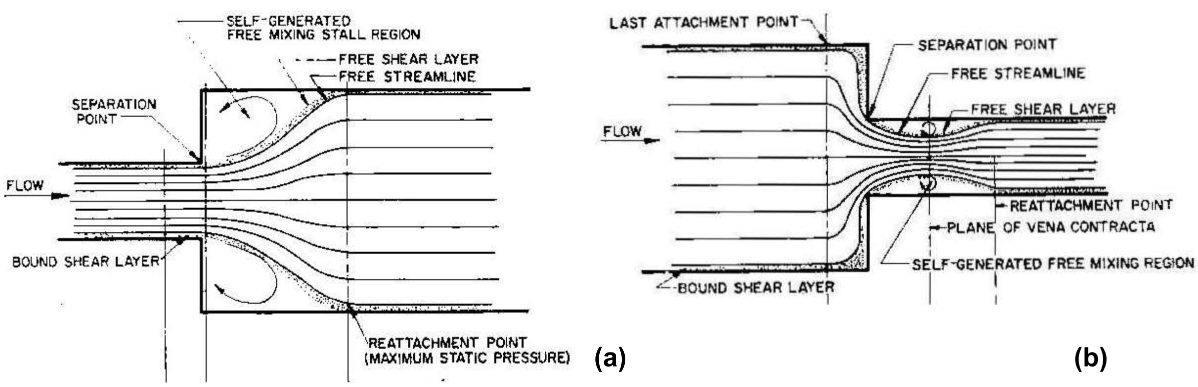

Fig. 7 Flow pattern at sudden expansion (a) or contraction(b)

The inlet losses due to sudden expansion (Fig. 7a) are easily calculated by the conservation of mass, momentum and energy between a small inlet section and the large cross section of the reactor- or heat exchanger- chamber. The well known Carnot-Borda equation

$$\Delta P = \frac{\rho\ (V_{in} - V_{out})^2}{2} \qquad (22)$$

is often used to describe the losses involved when a constant density flow encounters an abrupt increase in the area of its system boundaries. When operating at low Mach number in helium one can neglect the change in density and the following expression for the total pressure drop as a function of the mass flow and change of cross section is obtained.

$$\Delta P(\dot{m}) = \dot{m}^2 \frac{R_G\, T_{in}}{2\, P_{in}} \left(\frac{1}{A_{in}} - \frac{1}{A_{chamber}}\right)^2 \qquad (23)$$

The following empirical expression is a good approximation of the maximum head loss when a constant density fluid encounters an abrupt decrease of the area of its boundaries (Fig. 7.b). It mainly accounts for the deceleration resulting from the abrupt enlargement downstream of the “vena contracta” at the inlet of the outlet duct.

$$\Delta P = 0.5\ \frac{\rho\, {V_{out}}^2}{2}$$

what can also be written as:

$$\Delta P(\dot{m}) = 0.5\ \dot{m}^2 \frac{R_G\, T_{in}}{2\, P_{in}} \frac{1}{{A_{out}}^2} \qquad (24)$$

A more detailed definition of the expansion and contraction losses can be found in [4].

Other losses and temperature changes in the heat exchanger- combustor or reactor volume depend on the detailed geometry, the operating- and boundary conditions.

2.5 Turbines

Adding the temperature rise and pressure losses in the heat exchanger(s), reactor and piping to the compressor outlet conditions P_2 and T_2 provides the turbine inlet conditions P_3 and T_3.

The turbine performance can be predicted in the same way as the compressor but starting from the turbine performance map and inlet flow conditions (Fig. 2b). It allows calculating the turbine exit pressure P_4 and T_4 as a function of the inlet temperature and pressure

The low-pressure side of the gasturbine (from the turbine exit to the compressor inlet for closed cycle gasturbines or from turbine outlet to atmospheric pressure for open gasturbines) can be calculated by the component models described before for pipes and volumes. They provide P_5 and T_5 .

2.6 Component matching

Matching of the components i.e. definition of the operating point will be illustrated for the single shaft, single compressor gasturbine shown on Fig. 4. It concerns a closed cycle gasturbine driving an electrical generator. This figure also shows the bypass valves V1 and V2 and inventory control system V3 and V6 (to be discussed later).

Once the performance of each component is calculated as a function of the mass flow, one can calculate the pressure and temperature variation along the flow path for a first guess of the mass flow. Results of such a calculation for three different mass flows are illustrated on Fig. 8 by the total pressure variation along the fluid path.

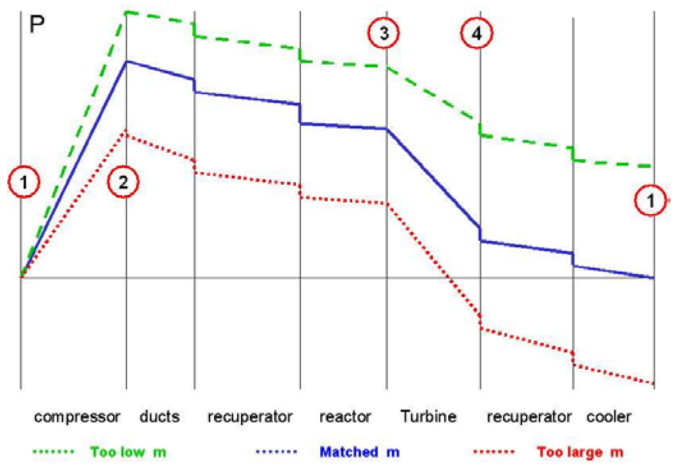

Fig. 8 Pressure variation along the flow path

Too low mass flow gives a too high ΔP in the compressor, a too low pressure drop in the ducts and volumes and a too low ΔP in the turbine. As a consequence the outlet pressure is higher than the inlet pressure. A too high mass flow give a too low ΔP in the compressor, followed by high friction and dump losses in the ducts and volumes and a too large ΔP in the turbine. The outlet pressure is too low. An iterative procedure is needed to find the correct mass flow.

In case of a closed cycle gasturbine, the same procedure should be used to find the temperature variation along the flow path, i.e. to verify if the final temperature at the cooler outlet (pos. 1) is the same as the one assumed when starting the cycle calculations. If not one should repeat the calculation of the temperature variation with this new compressor inlet temperature until the starting and final value of the temperature are the same.

The power available at the electrical generator is:

$$KW_E = KW_T - KW_C - KW_{aux} \qquad (25)$$

An iterative approach, as described in [3], in which the mass flow is iteratively adjusted is the appropriate way to solve the problem in a computerized way.

Vavra gives a graphical solution to the matching problem [5]. A simplified version, accounting only for the compressor and turbine performance map is illustrated on Fig. 9. It graphically defines the point where at given RPM the compressor pressure rise, corrected for the pressure drop between compressor and turbine, equals the turbine pressure drop for the corresponding mass flows. The solution is more readily obtained by the intersection points of the corresponding speed lines, when superpositing the two performance maps (Fig. 10).

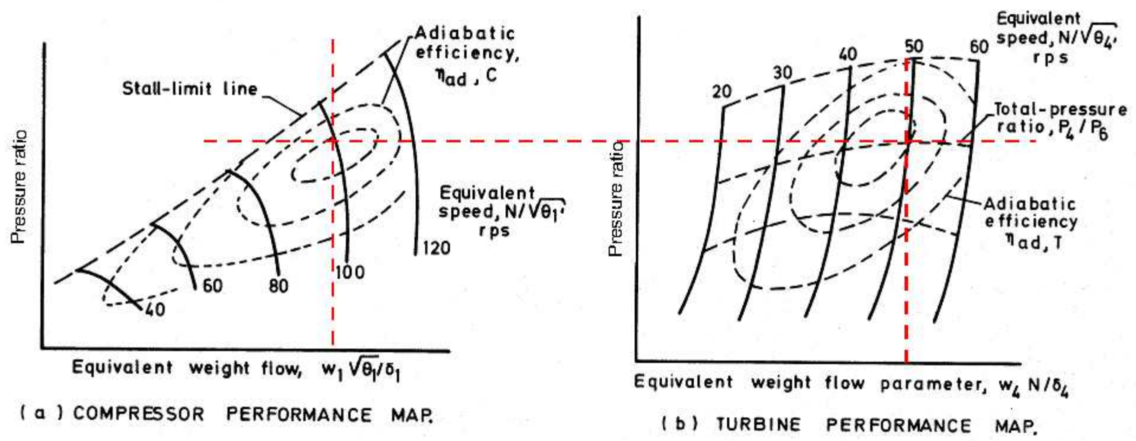

Fig. 9 Graphical solution of matching problem.

Figure 10 shows the compressor and turbine performance curve (at constant RPM) for different inlet pressures. It shows the pressure rise/drop versus mass flow for given inlet pressure and temperature of compressor and turbine at the same mechanical rotational speed (derived from the appropriate equivalent rotational speed curve). The simplified approach allows a better understanding of the change in performance for changing operating conditions i.e. change in pressure level in the closed gasturbine.

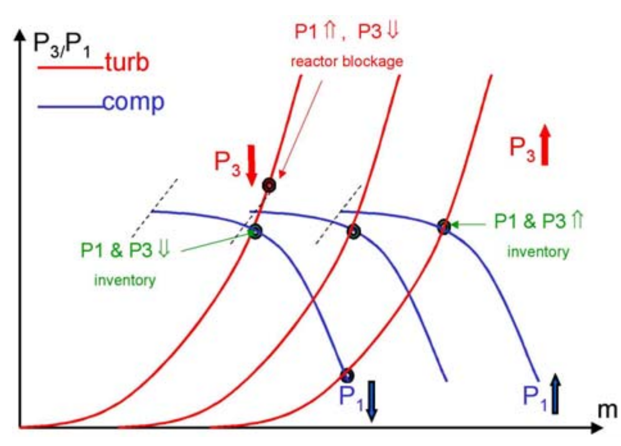

Fig. 10 Variation of operating point with pressure level

Matching of the compressor and turbine is at the intersection of the compressor- with the turbine pressure versus mass flow curve.
An increase of the inventory results in:
* a higher pressure at both the compressor and turbine inlet (**P1** and **P3** ⇑)
* a constant pressure ratio because it is independent of inlet pressure
* an increase of mass flow increases with the inlet pressure (fluid density) which results in an equivalent increase of the power output.
A decrease of the inventory results in a lower pressure at compressor- and turbine inlet and hence a lower mass flow and power (**P1** and **P3** ⇓). The operating points corresponding to the different inventories are all in the stable region.

An increase of the compressor inlet pressure combined with a decrease of the turbine inlet pressure (**P1**⇑ and **P3** ⇓). (because of increased pressure losses in the recuperator or reactor blockage) will push to compressor to an unstable operating point (left of the compressor surge limit).

A decrease of the compressor inlet pressure (**P1**⇓). in combination with an increase of the turbine inlet pressure (**P3**⇑) will result in a more stable operating point near compressor choking.

PART II – GASTURBINE TRANSIENT OPERATION

Previous approach is valid only if every component is operating at steady conditions i.e. if all changes in operating conditions are sufficiently slow so that the flow can adapt itself to the new condition and the performance of each component is the one corresponding to the steady operating curves.

The transient operation of an open gasturbine (jet engine) compressor is illustrated on Fig. 11 a and b for an acceleration or deceleration. The main difference between this geometry and a closed cycle gasturbine driving an electrical generator is the non-constant RPM and near choking operation of the turbine (no increase of the mass flow at decreasing outlet pressure).

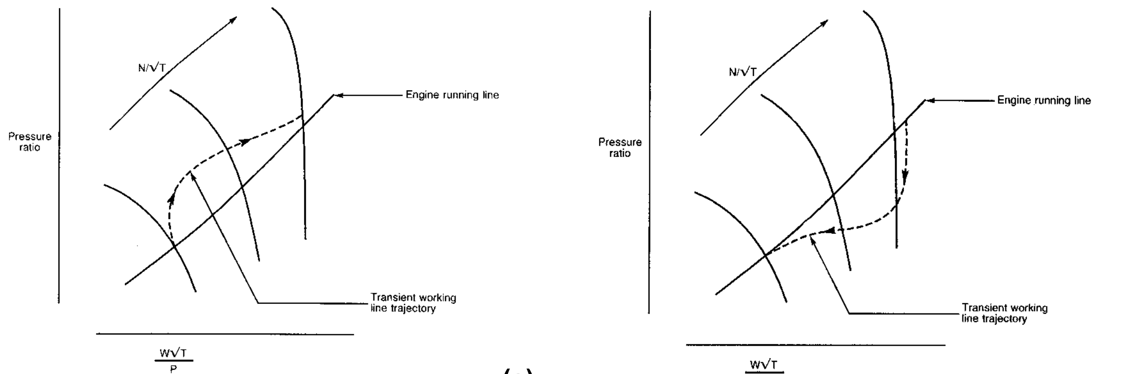

(a) (b)

Fig. 11 Transient flow path at acceleration or deceleration.

An acceleration is obtained by an increase of the turbine inlet temperature (increased fuel flow) (Fig. 11a). Since for a choked turbine the value of $\dot{m}\frac{\sqrt{T}}{P} = \dot{m}_{ref}\frac{\sqrt{T_{ref}}}{P_{ref}} = C_{te}$, the turbine inlet pressure will rise with the square root of the inlet temperature. Depending on the geometry, the compressor mass flow may decrease along the constant speed line, to compensate for the increased back pressure, until the RPM increases. This increase of RPM is the consequence of a larger power output by the turbine when increasing the inlet temperature.

The consequence is a new operating point at higher RPM. The time needed to increase the RPM depends on the extra torque generated by the turbine and the inertia of the rotor. The main risk is that the compressor operating point may move beyond the surge line in the unstable area. A sufficiently large safety margin between the operating point and the surge line must therefore be respected. Previous arguments could be refined by accounting also for the temporary accumulation of mass flow in the volumes between compressor and turbine.

The opposite occurs when reducing the fuel flow (Fig. 11b). The turbine inlet temperature decreases resulting in a decrease of the compressor back pressure and the compressor operating point shifts to choking conditions. The decrease of torque and RPM finally results in a new operating point at lower mass flow. This change in operation bears almost no risk for unsteady operation (Fig. 11b).

The required compressor surge margin depends on the slope of the turbine performance curve. Helium turbines operate at very low Mach number and do not suffer from choking at Mach 1. A decrease of the turbine outlet pressure quickly results in an increase of mass flow and a smaller shift along the compressor operating line (Fig. 12 a versus b). However the situation is worsened by the constant RPM of closed cycle gasturbine. The temporary increase in compressor pressure rise, needed to compensate the increased pressure drop in the turbine must be fully compensated by a shift along the compressor operating line at constant RPM. This may increase the required large safety margin.

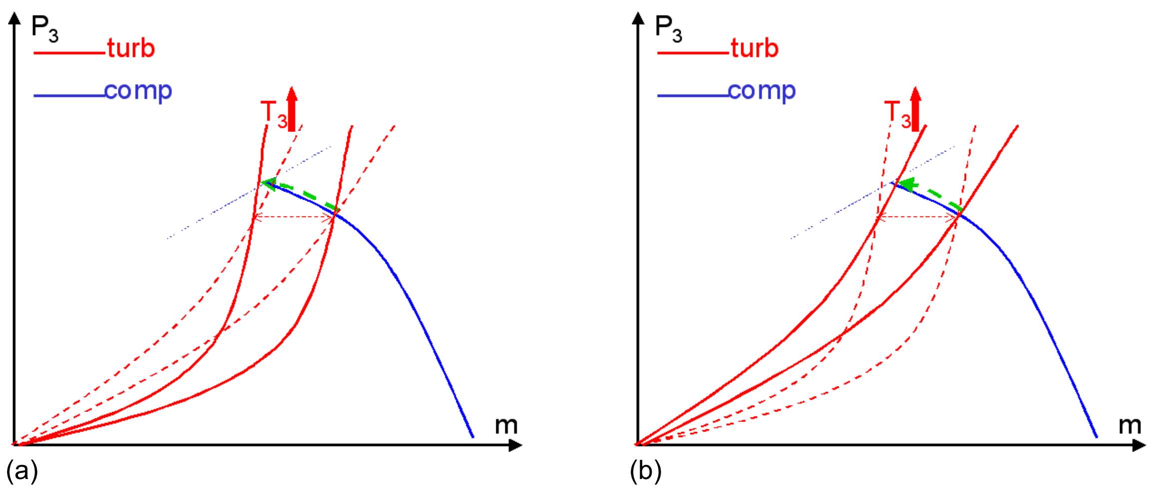

Fig. 12 Compressor surge margin for a choked (a) or unchoked (b) turbine

Transients may occur in a closed gasturbine when:

1. the compressor inlet temperature increases because the water supply to the inlet cooler drops out.
2. the turbine inlet temperature changes due to a sudden change in reactor heat supply (emergency stop or reduced mass flow).
3. the compressor inlet pressure increases because of opening the bypass or change in inventory (Fig. 4).
4. the turbine inlet pressure changes because of opening or closing the bypass valve.

Many other abrupt changes of operating conditions may occur and should be experimentally or theoretically analyzed to guarantee a safe and stable operation.

Different time scales govern the transient operation. They depend on the geometry and propagation speed of the perturbations.

1. pressure changes propagate with the speed of sound and result in time scales well below 1 sec. They mainly govern the inertial effects.
2. mass accumulation in volumes and change of rotational speed occur at time scales of 1 second and higher.
3. thermal inertia and heat soaking (heating/cooling of the gas by the heat/cold accumulated in the thick walls) have time scales up to 10 sec.

A correct prediction by the unsteady flow modeling and experimental facilities can be guaranteed only if these differences in time scale are respected.

Typical performance maps of a compressor and turbine operating at low Mach number are shown on Fig. 13 and 14. The speed line at .775 RPM_{ref} is similar to the performance map of the Helium compressors and turbine predicted in [8]. The compressor map shows a rather large operating range and one can assume that the turbine is unchoked. More precise predictions are presented in deliverable n^o 9 of WP 1 [8].

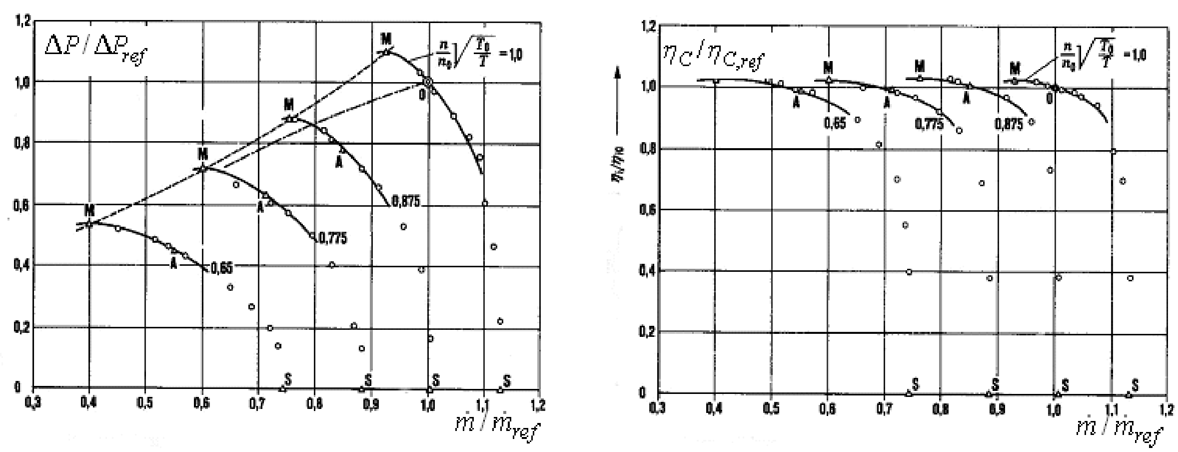

Fig. 13 Typical performance map of a compressor operating at low Mach number [3].

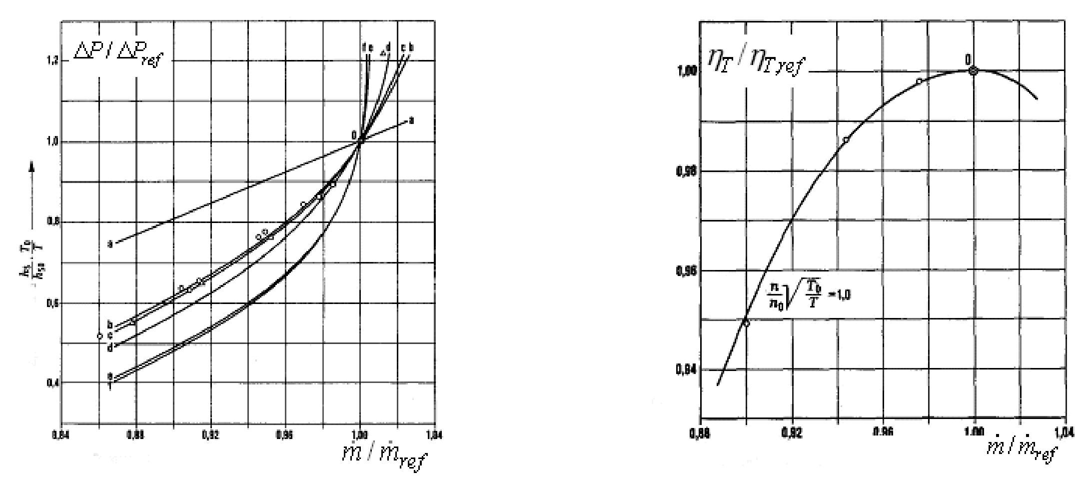

Fig. 14 Typical performance map of a turbine operating at low Mach number (curves a to f correspond to different approximated predictions) [3].

1. Modeling

The modeling calculates the change in mass flow and energy flux in each component of the gasturbine under the influence of an non equilibrium between the pressure- and temperature change in each component and the instantaneous inlet and outlet values. It makes use of the schematic lay-out of the gasturbine shown in Fig. 4.

The mass flow at the inlet/outlet of each component equals the mass flow at the outlet/inlet of the previous/next component. However the instantaneous value of the mass flow does not need to be the same all along the gas path i.e. fluid can accumulate in volumes so that the outflow can be temporarily different from the inflow.

The pressure and temperatures are the same on both sides of the interfaces but can be different from interface to interface.

1.1 Ducts

The equation describing the steady flow pressure drop in a duct can easily be extended to unsteady flows by adding the inertial term corresponding to the acceleration or deceleration of the mass of fluid contained in the duct (Fig. 15). This extension does not account for the unsteady pressure wave propagation and is strictly spoken valid only for incompressible flows (solid column theory).

$$\Delta P = C_f \ \rho \ V^2 \frac{L}{D_H} + \frac{L}{A} \cdot \frac{d\dot{m}}{dt} \qquad (26)$$

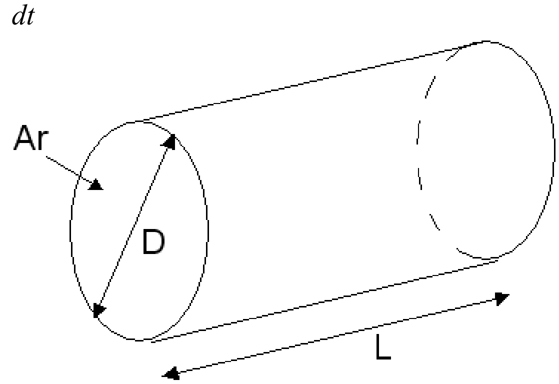

Fig. 15 Duct flow

The temperature change from inlet to outlet is defined in the same way as for steady flows (eq. 13 to 16) as a function of the heat flux corresponding to the instantaneous wall temperature.

1.2 Compressor

One assumes that the volume of the compressor is too small to accumulate mass in a significant amount. The outlet mass flow equals the inlet mass flow at all moments.

$$\dot{m}_{C,in} = \dot{m}_{C,out} \tag{27}$$

The mass flow in the compressor will increase of decrease if the pressure rise corresponding to the instantaneous mass flow $\Delta P_C(\dot{m}_C)$ (defined from Fig. 13) is different from the instantaneous pressure difference that is applied between the compressor inlet and outlet $(P_{out} - P_{in})$. This unbalance of pressure is applied to the cross section area Ar_C, over a distance equal to the compressor length L_C and results in an increase of the fluid velocity (and hence of mass flow) in a way similar to the acceleration of a fluid in a duct (Fig. 15).

$$\frac{L_C}{Ar_C}\frac{d\dot{m}_C}{dt} = \Delta P_C(\dot{m}_C) - (P_{out} - P_{in}) \tag{28}$$

$\Delta P_C(\dot{m}_C)$ is readily obtained from the compressor performance map (Fig. 13) assuming that the unsteady compressor performance equals the steady one.

The corresponding change in temperature is function of $\Delta P_C(\dot{m}_C)$ and efficiency

$$T_{out} - T_{in} = \Delta T_C = T_{in} / \eta_C \cdot \left((1 + \Delta P_C / P_{C.in})^{\frac{\gamma-1}{\gamma}} - 1 \right) \tag{29}$$

1.3 Turbines

The variation of the flow in the turbine is calculated in a way similar to the one explained for the compressor. It assumes no difference between the inlet and outlet mass flow.

$$\dot{m}_{T,in} = \dot{m}_{T,out} \tag{30}$$

and a fluid acceleration driven by the unbalance in pressure drop

$$\frac{L_T}{A_T}\frac{d\dot{m}_T}{dt} = (P_{in} - P_{out}) - \Delta P_T(\dot{m}_T) \tag{31}$$

The temperature change can be expressed as a function of the pressure drop and efficiency.

$$T_{in} - T_{out} = \Delta T_T = \eta_T . T_{in} \cdot \left(1 - (1 - \Delta P_T / P_{in})^{\frac{\gamma-1}{\gamma}} \right) \tag{32}$$

Input is from graphs like the ones shown on Fig. 14

1.4 Volumes

Temporarily differences between the in- and outflow of volumes results in an accumulation/decrease of fluid in the volume. At constant volume it requires an increase/decrease in density in the volume defined by:

$$\frac{d\rho}{dt} Vol = \dot{m}_{in} - \dot{m}_{out} \tag{33}$$

and hence results in following change of pressure in the volume.

$$\frac{dP}{dt} = \frac{d\rho}{R_G.T} = \frac{\dot{m}_{in} - \dot{m}_{out}}{R_G.T.Vol} \tag{34}$$

The velocity being very small there is no pressure gradient in a volume and the same average pressure is imposed at inlet and outlet section of the volume.

The heat balance between incoming and outgoing flow and the heat flux through the walls provides the change of average fluid temperature in the volume.

$$\frac{dT}{dt} = \frac{\dot{m}\,T_{in} - \dot{m}\,T_{out}}{\rho\,Vol} + \frac{\dot{Q}_{wall}}{\rho\,Vol} \tag{35}$$

$\dot{Q}_{wall}$ stands for the heat flux between the wall and the fluid in the volume when the wall temperature is different from the fluid temperature (heat soaking). The instantaneous heat flux is calculated in the same way as explained in 2.2

The hot ducts are internally isolated and, depending on the porosity and thickness of the isolation, they may behave as extra volumes because the fluid and heat absorption in the isolation may no longer be negligible (Fig. 16).

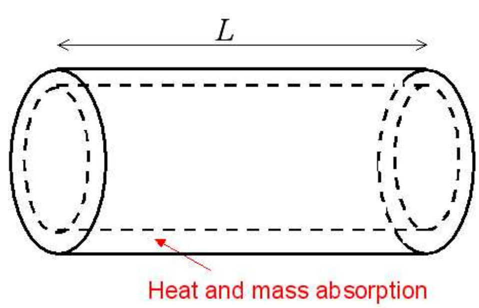

Fig 16. Isolated ducts

1.5 Heat exchangers

Depending of the geometry the unsteady behavior of heat exchangers should be treated in the same way as volumes, where flow can accumulate, or as ducts where an inertial term must be added. Temperatures should be the instantaneous wall temperature.
The off-design operating curves, shown on Fig. 5 and 6, can be used to provide a quick prediction.

1.6 Solution procedure

Starting from an initial situation (pressure, temperature and mass flow in each interface and given RPM) one can calculate the time evolution of the flow by a time integration of the equations defining the change in mass flow (eq. 26, 28 and 31), pressure (eq. 34) and temperature (eq. 29, 32 and 35) until a steady situation is reached. Underrelaxation may be needed for that. This procedure allows verifying if the compressor flow remains stable, if thermal shocks occur in the ducts and volumes and what are the changes in RPM.

2. Examples

Following discusses examples illustrating some typical unsteady operations of gas turbines. The first ones are obtained on a 3 compressor single shaft closed cycle gasturbine schematically shown on Fig. 17. The others are obtained on the Oberhausen Helium turbine shown on figure 21. They are discussed here in order to reach a better understanding of the transient phenomena that can occur in closed cycles and to find out what studies may be needed.

2.1 Change of inventory

Bammert [6] has studied the unsteady flow in a single spool, three compressor 25 MWe closed cycle gasturbine operating in helium. The lay-out is schematically shown on Fig. 17.

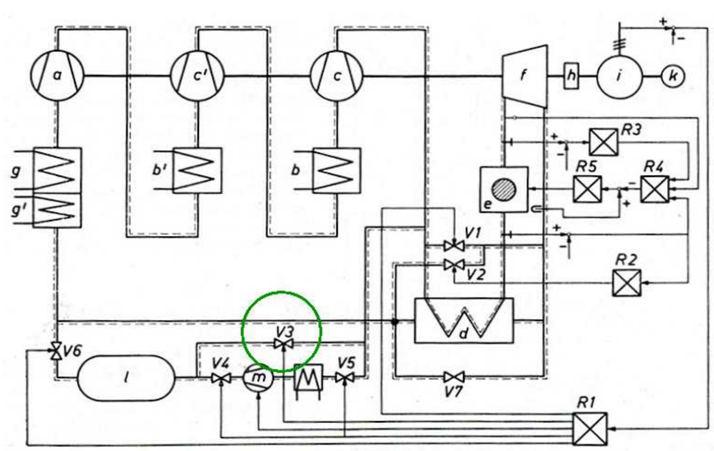

Fig. 17 Single spool, three-compressor closed cycle gasturbine

The predictions assume a constant inlet temperature and constant temperature difference at the exit of each heat exchanger. The reactor dynamics are excluded and the reactor outlet temperature is kept constant. The results of simulating a decrease in inventory by opening valve V3 to generate a 3%/sec of the initial fluid quantity in the closed gasturbine decrease is shown on Fig. 18.

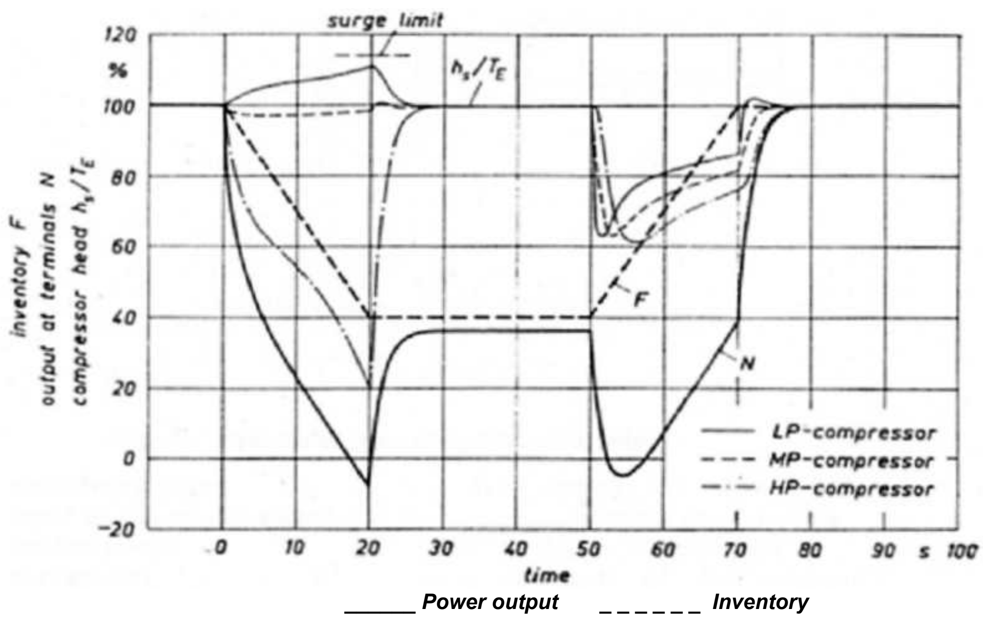

Fig. 18 Variation of Compressor Head, Electrical Output and Inventory

The inventory *F* decreases linearly to 40% of its initial value in 20 sec. Extracting working fluid from the HP side, the turbine inlet pressure drops and the electrical power output rapidly decreases to less than zero in the same time interval. It is followed by a gradual increase to the steady value corresponding to a 40% inventory once the amount of fluid in the circuit is kept unchanged. One observes that the power decrease is proportional to the amount of gas in the circuit.
The HP compressor pressure rise rapidly drops to 20% of its design value because the extraction takes place at its output section. The LP compressor pressure rise increases to close to the surge limit and returns to the design pressure ratio after 20 seconds. It would exceed the surge limit for an inventory changing rate larger than 3%/sec.

Fig. 18 also shows the consequences of repressurizing the gasturbine by reinjecting the fluid at the LP side (V6) at a rate of 3%, starting at t=50 sec.. The initial dip of the electrical power output results form the fact that the three compressors require additional power to compress the extra gas before the turbine delivers the extra power required by the compressors. This dip in power output increases with increasing feeding rate. All compressors operate well away from their surge limit.

The consequences of repressurizing the gasturbine by injecting the fluid at the compressor HP side (opening V3 with an extra compressor) are shown on Fig 19 for a feeding rate of 1%/sec. It results in an immediate increase of the power output at the same rate as the increase in inventory. However , the rapid increase of the pressure at the exit of the HP compressor drives it towards the surge limit. And a feeding rate in excess of 1% would put the HP compressor into surge. A safe increase of inventory, when injecting at the HP side, takes 60 seconds versus 20 seconds for a feeding at the LP side.

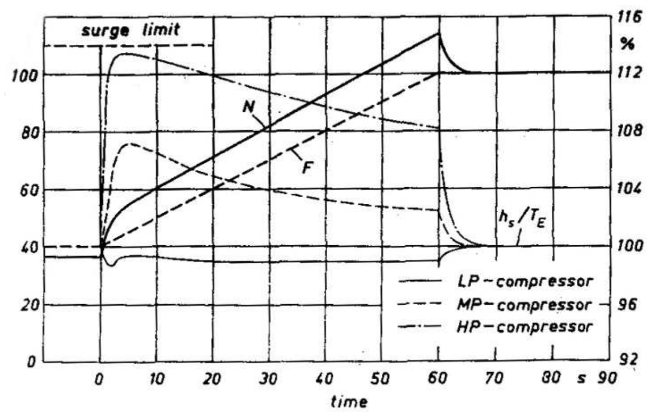

______ Power output _ _ _ _ _ _ Inventory

Fig. 19 Increase of inventory by injecting on the HP side.

Figure 20 shows the power output and pressure variation at the LP and HP side of the compressors when opening the valves V1 and V2 just enough to cause the power output to become zero. A more rapid decrease of power output in case of emergency may require large valves

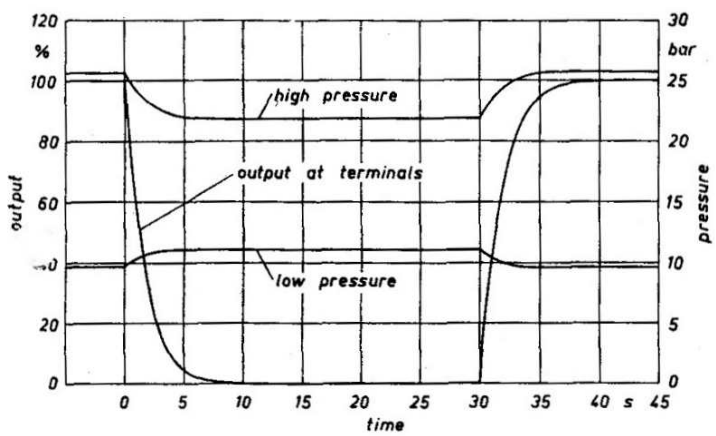

Fig. 20 Bypass valve opening

2.2 Emergency stop

The theoretical study of the operating behavior of the Oberhausen Closed-cycle Helium turbine during emergency shut down is described in [7]. The emergency shut down, usually used for closed cycle air turbines, by discharging the circuit inventory to the atmosphere, can not be applied to helium for cost reasons. Instead, in the event that an emergency stop is required, the by-pass valve (p) is fully opened (Fig. 21). This valve is rated to reduce the pressure ratio of the facility to 1 in a few seconds and the gasturbine to be stopped after a short time. A schematic view is shown on Fig. 21. In order to limit the thermal shock in the recuperator (d), because of the increased turbine outlet temperature, one also opens the valve (o)

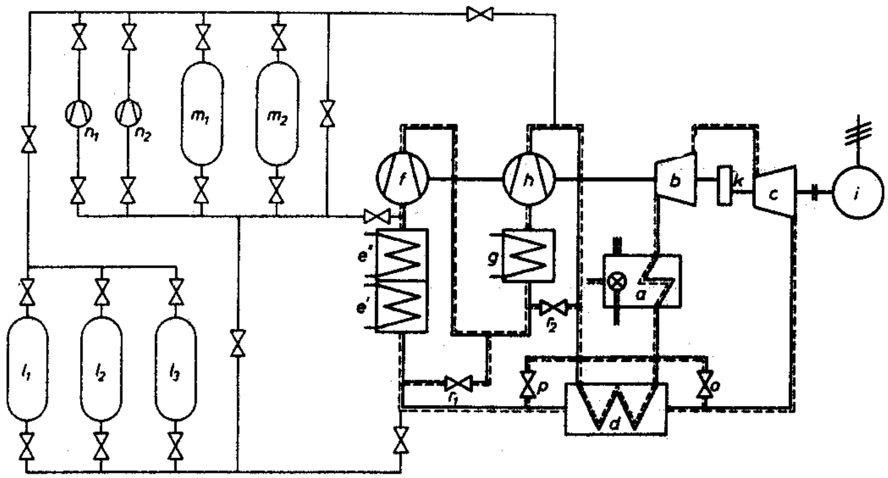

Fig. 21 Lay out of the Oberhausen Helium Closed Cycle Gas-Turbine

Fig. 22 shows the control process for a full load release at time 0 . One observes a maximum overspeed of 7% after 2 seconds and a return to nominal after 7 seconds. The power at the gear box (k) between LP and HP turbine increases from 50 to 63 % of the electrical power output.
Reconnecting the load after 17.5 seconds results in a 4% drop of RPM.

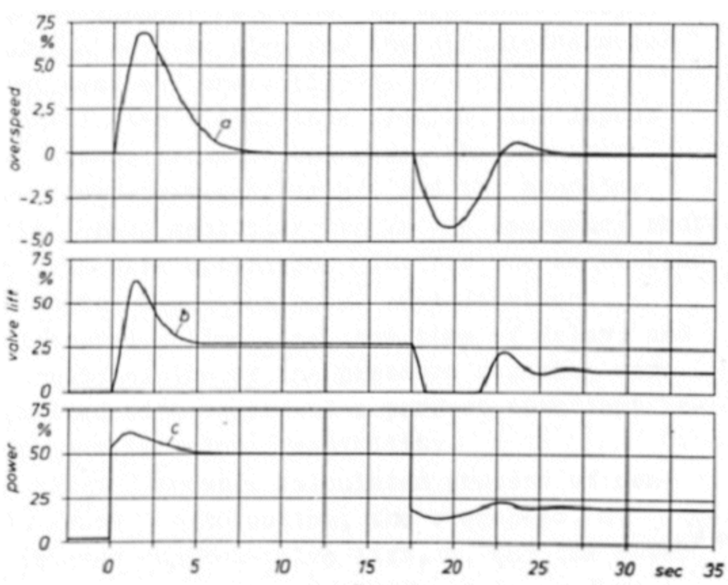

Fig. 22 Variation of RPM and gear box power at full load release

The results of a dynamic calculation of an emergency shut down at nominal speed is shown on Fig. 23. At time t=0 the alternator is disconnected, the heater is stopped and the emergency valve is fully opened. The speed (a) drops to 27% in 30 seconds, the mass flow (b) at the heater outlet decreases to about 8%, The pressure upstream (c) and downstream (d) of the two turbines quickly approach an equilibrium value of 14.6 bar. Although the heater is turned off immediately, its outlet temperature (e) remains high because of the heat soaking in the heater at reduced mass flow. The turbine outlet temperature (f) rises more slowly than the turbine pressure balancing process because of the large thermal capacity of the turbines. It is shown in [7] that the layout temperature is never exceeded nor has it an unacceptable gradient.

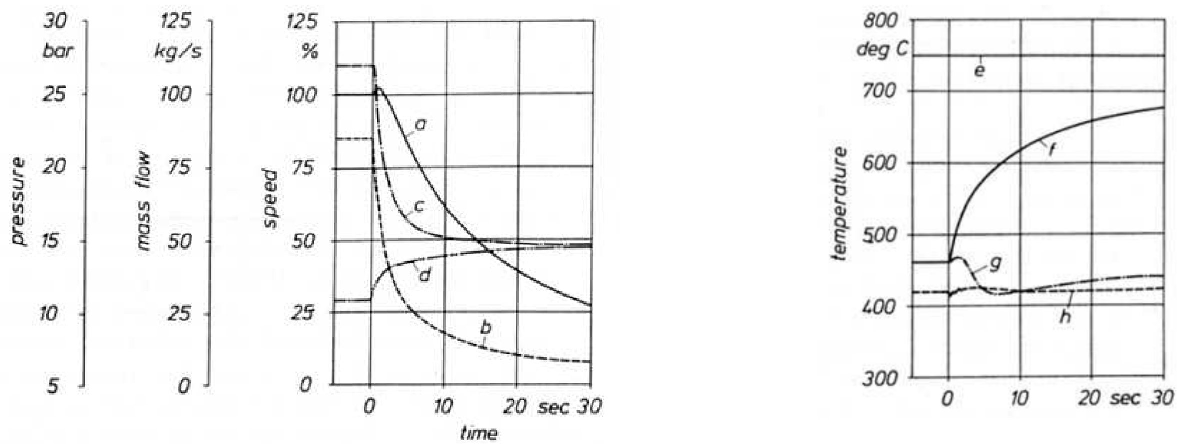

Fig. 23 Emergency shut down

PART III – HELIUM TESTING IN THE HTR-10GT FACILITY

The HTR-10GT presently under construction by INET at the Tsinghua University in PRC is a smaller (2. 07 MW electric power) closed cycle gasturbine operating with Helium and heated by a nuclear reactor. It is an extension of the HTR-10 reactor operating with a heat exchanger. All data are obtained from the flow diagram shown on Fig. 24 [9].

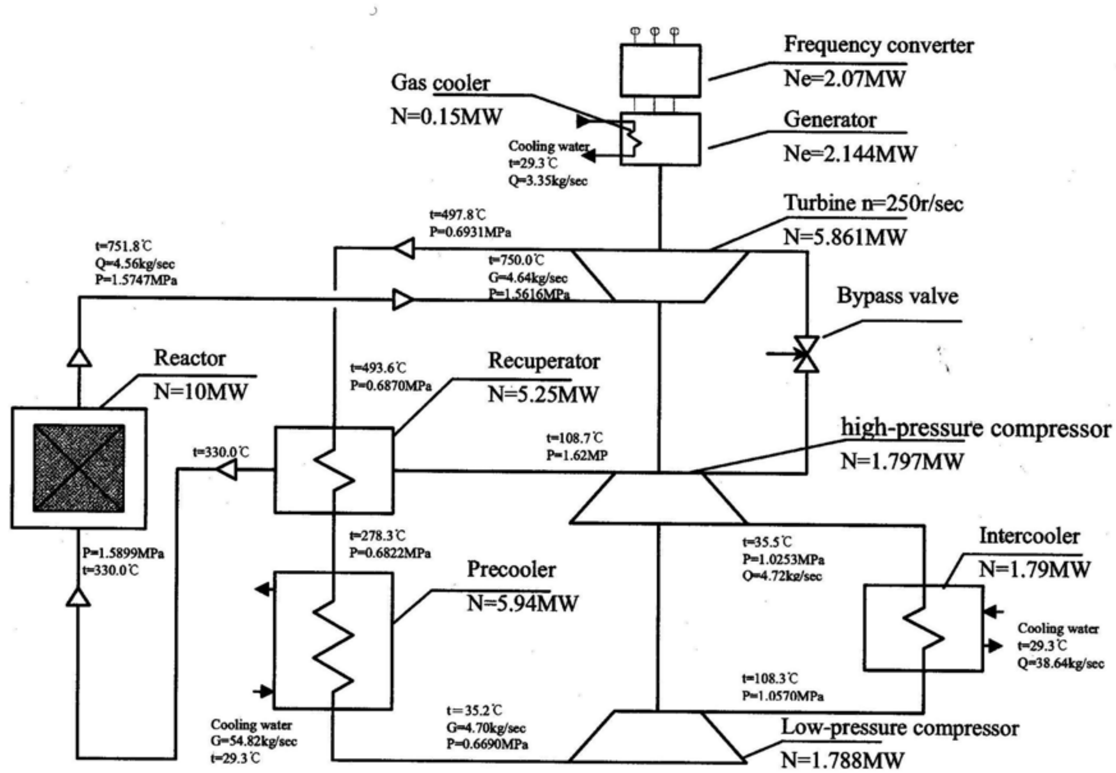

Fig. 24 Flow diagram of the HTR-10GT

No information is provided about the dimensions of the turbomachinery components. However the thermodynamic information that is provided allows a rather good estimation on how those components should look like. Two approaches are followed to find out in how far this facility could be used for the development of the HTR-E turbomachines:

1. Analysis of the possibility to do turbomachinery performance testing in that facility by replacing the turbomachines of the HTR-10GT by scaled models of the compressors and turbine designed and studied in Part I and II i.e. how far are the flow conditions different from the ones of HTR-E.
2. Verifying in how far the turbomachinery components of the HTR-10GT could be considered as scaled models of the HTR-E turbomachinery components proposed in Part I and II. Question is if the performance of those components are relevant for our application, and if they can be used to verify and calibrate the design and analysis tools that have been used in present design.

1. Turbine performance

The HTR-10GT turbomachinery components are smaller and operate at *15 000. RPM* instead of *3 000. RPM* for the HTR-E ones. This requires calculating a "scaled model" in a way similar to what is explained in 1.1 and 1.2 .

Results of the turbine performance and flow characteristic estimations for the turbine are summarized in Table 2.

- The performance of the full scale HTR-E turbine is listed in line 1.
- The characteristics of the turbine scaled according to section 1.1 and 1.2 are listed in line 2.
- The best estimation of the characteristics of the HTR-10GT turbine, based on the information available on Fig. 24, are listed in line 3.

Table 2. Turbine scaling results

RPM	Diameter	chord	Re	η	ΔH	ΔT	Mass fl.	Power
3000	1.9	0.06	1195587	0.903	1716758	330.4	318.5	546 787 550
15000	0.36	0.012	53344	0.903	1566397	301.5	2.7	4 252 450
15000	0.38	0.012	55845	0.888	1308872	251.9	4.6	5 968 458

Tin	Tout	Pin	Pout
1121	790.8	7000000	2606865
1023	721.5	1561600	581554
1023	771.1	1561600	693100

The first observation is the small turbine diameter and chord length at 15 000. RPM. This results in a very low Reynolds number. It means that the efficiency of the scaled models could be much lower than for the full scale HTR-E geometry. Based on the thermodynamic data provided on Fig. 24, the HTR-10GT turbine efficiency was estimated at 88.8% instead of 90.3% for the HTR-E turbine. This reduction in efficiency is small considering the rather large change in Reynolds number. Special actions may be needed to avoid flow separation on the last stages of the turbine of the HTR-10GT turbine (lowest pressure and Reynolds number). The mass flow of the HTR-10GT turbine is 50% larger then the one of the scaled turbine. This results in almost 50% larger power output for the HTR-10GT turbine. It also means that the blades will be 50% longer. It is likely that also the blade chord has been increased proportionally to avoid a too large aspect ratio. This likely increase of the chord means a 50% increase in the Reynolds number and can explain the rather small difference between the predicted full scale HTR-E and HTR-10GT turbine efficiency derived from Fig. 24.
Nothing can be said about the blade loading because the blade number and number of stages is not specified. Hence, its impact of blade loading on efficiency cannot be evaluated.

One can conclude that:

- the HTR-10GT facility provides the thermodynamic conditions needed to test a scaled model of the HTR-E turbine but that corrections for Reynolds number changes will be needed.
- The operational conditions and performance of the HTR-10GT turbine are similar to the ones of the HTR-E turbine and experimental results may be used to validate the numerical prediction methods used for the HTR-E design at very realistic conditions.

2. Compressor performance

Results of the compressor performance and flow characteristics estimation are summarized in table 3.

- The performance of the full scale HTR-E LP compressor at *3000 RPM* are listed in line 1.
- The characteristics of the LP compressor, scaled according to the theory explained in section 1.1 and 1.2 to operate at *15 000 RPM* are listed in line 2.
- The best estimation of the characteristics of the HTR-10GT HP compressor, based on the information available on Fig. 24, is listed in line 3.
- The best estimation of the characteristics of the HTR-10GT LP compressor, based on the information available on Fig. 24, is listed in line 4.

Table 3. Compressor scaling results

RPM	Diameter	chord	Re	η	ΔH	ΔT	Mass fl.	Power
3000	1.80	0.060	1547228	0.940	404301	77.81	318.5	128 769 792
15000	0.36	0.012	81184	0.940	394836	75.99	3.30	1 304 150
15000	0.37	0.012	124421	0.842	381906	73.50	4.72	1 802 596
15000	0.37	0.012	81184	0.896	381906	73.50	4.70	1 794 958

Tin	Tout	Pin	Pout
299.0	376.8	2550000	4409030
292.0	368.0	669000	1156722
308.5	382.0	1025300	1620000
308.5	381.6	669000	1083000

The increase in RPM results again in a large decrease of the diameter and chord length and hence in a decrease of the Reynolds number well below its critical value. The HTR-10GT LP compressor efficiency is 5% points lower than the HTR-E estimation. It is very surprising that the HP efficiency of HTR-10GT is even 10 % points lower because the Reynolds number at the inlet is higher and already close to the critical value. It will even increase above that value further downstream in the compressor. This large decrease of the HP compressor efficiency could be the consequence of the very small compressor dimensions and the difficulty to respect the tight manufacturing tolerances that are required in that case.

The mass flow of the HTR-10GT is again 50% larger than for the scaled LP and HP compressors. The HTR-10GT compressors geometry could be very similar to the scaled LP and HP ones if also the chord is increased by 50%.
Nothing can be said about the blade loading because the number of blades and stages is not specified.

One can conclude that:

- the HP compressor part of the HTR-10GT facility provides the thermodynamic conditions needed for an accurate test of a scaled model of the HTR-E compressor and that corrections for Reynolds number changes may not be needed. The LP compressor part of the HTR-10GT facility is much less suited for that testing because of a too low Reynolds number.
- The lay-out of the HTR-10GT compressor is similar to the HTR-E compressor and the HP compressor experimental results may be used to validate numerical prediction methods under conditions that are very similar to the compressors of the HTR-E facility.

CONCLUSIONS

The models, that have been presented, allow defining the conditions for a correct experimental simulation of the steady and unsteady phenomena.

A change in density of the fluid should not violate the similarity because both mass flow and pressure scale with the density.
A change in pressure level may be needed to keep the Reynolds number sufficiently high to correctly simulate the losses.
A change in the speed of sound should result in a proportional change in peripheral and fluid velocity to correctly simulate the compressibility effects.

The models can be used to predict the unsteady behavior of a closed cycle gasturbine during transients (change of load) as well as during emergency and accidental changes of the boundary conditions.
Main requirements are:

- a model compressor/turbine performance map that is similar to the one of the real compressor/turbine.
- conservation of the ratio between the different volumes of reactor, heat exchangers and coolers.

conservation of the length over area ratio of the ducts.

However it is not required that an experimental setup simulates exactly every component of the closed cycle gasturbine. Any difference between the full scale geometry and the down scaled model can be accounted for by changing the appropriate parameter in the analysis model. The experiments are used only to verify the validity of the prediction models.

The HP compressor part of the HTR-10GT facility provides the thermodynamic conditions needed for an accurate test of a scaled model of the HTR-E compressor. The HTR-10GT LP compressor and turbine are much less suited for that kind of testing because of a too low Reynolds number.

The lay-out of the HTR-10GT compressor and turbine are similar to the HTR-E compressors and turbine. The HP compressor experimental results may be used to validate numerical prediction methods under conditions that are very similar to the HP compressor part of the HTR-E facility. Some caution is needed when using the experimental results of the LP compressor and turbine for validation of the design and analysis codes because of the Reynolds number of the experiments is below or close to the critical value.

A word of caution: One should verify in how far the tolerances have been respected when downsizing the geometries.

BIBLIOGRAPHY.

[1] Colebrook, C.: Turbulent Flow in pipes with particular reference to transition region between the smooth and rough pipe laws. Journal of the Institute of Civil Engineers London, 11 (pp. 133-156), 1939

[2] Dittus F.W. & Bölter,: University of California Publications on Engineering 2 (1930), p. 433.

[3] Bammert K. & Twardziok W.: Das stationaire Betriebsverhalten von konventionelle- und nuklearbeheitzten Gasturbinen, Atomkernenergie 11 jg 1966 heft 5/6 (pp. 185-204)

[4] Benedict R.P., Carlucci N.A. and Swetz S.D.: Flow losses in Abrupt enlargements and Contractions, ASME Trans., Journal of Engineering for Power, January 1966, (pp73-81)

[5] Vavra M.: A graphical Solution of the Matching Problem in Closed Cycle Gas Turbine Plants, ASME paper 66-GT/CLC-14, ASME transactions, Journl. of Engrg. for Power

[6] Bammert K. and Krey G.: Dynamic Behavior and Control of Single-shaft Closed-Cycle Gas Turbine, ASME trans., Journal of Engineering for Power, October 1971, (pp. 447-453)

[7] Bammert K, Krey G. and Krapp R.: Operation and Control of the 50 MW Closed Cycle Helium Turbine Oberhausen, ASME paper 74-GT-13

[8] Van den Braembussche R.A., Aerodynamic Design –CFD calculations, Deliverable 9 of WP1, HTR-E 05/08 D-1-2-2

[9] Yuanhui Xu, Status of the HTR program, Institute of Nuclear and New Energy Technology, Tsinghua University, 2005